

# A photographic method for drop characterization in agricultural sprinklers

by

Salvador, R.<sup>1</sup>, Bautista-Capetillo, C.<sup>2</sup>,

Burguete, J.<sup>1</sup>, Zapata, N.<sup>1</sup>, Serreta, A.<sup>3</sup> Playán, E.<sup>1</sup>

## ABSTRACT

The characterization of drops resulting from impact sprinkler irrigation has been addressed by a number of techniques. In this paper, a new technique based on low-speed photography (1/100 s) is presented and validated. The technique permits to directly measure drop diameter, velocity and angle. The photographic technique was applied to the characterization of drops resulting from an isolated sprinkler equipped with a 4.8 mm nozzle and operating at a pressure of 200 kPa. Sprinkler performance was characterized from photographs of 1,464 drops taken at distances ranging from 1.5 to 12.5 m. It was possible to analyze separately the drops emitted by the main jet and those emitted by the impact arm. The proposed technique does not require specific equipment, although it is labour intensive.

**Keywords:** impact sprinkler, drop, diameter, velocity, angle, photography, low-speed.

---

<sup>1</sup> Dept. Soil and Water, Aula Dei Experimental Station, CSIC. P.O. Box. 202, 50080 Zaragoza, Spain. rsalvador@eead.csic.es, jburguete@eead.csic.es, vzapata@eead.csic.es, enrique.playan@eead.csic.es

<sup>2</sup> Dept. Planeación de Recursos Hidráulicos, Universidad Autónoma de Zacatecas. Avda. Ramón López Velarde, 801. Zacatecas, Zacatecas, México. baucap@uaz.edu.mx

<sup>3</sup> Escuela Politécnica Superior de Huesca, Universidad de Zaragoza. Ctra. de Cuarte, s/n, 22071. Huesca, Spain. serreta@unizar.es.

## 21 INTRODUCTION

22 The characterization of drops resulting from impact sprinkler irrigation typically implies  
23 the determination of their diameter as they approach the soil surface. Drop  
24 characterization has been used for different purposes related to irrigation management,  
25 such as evaporation losses, soil conservation and irrigation simulation. Evaporation  
26 losses have often been empirically correlated with wind speed (Edling 1985; Trimer  
27 1987; Keller and Bliesner 1990; Tarjuelo et al. 2000; Playán et al. 2005). Wind speed  
28 has been found to affect fine drops much more than large drops (Fukui et al. 1980;  
29 Thompson et al. 1986, De Lima et al. 1994; De Lima et al. 2002). Lorenzini (2006)  
30 presented a theoretical analysis of water droplet evaporation, and stressed the  
31 importance of air friction and air temperature on the process. Regarding soil  
32 conservation, drop kinetic energy results in soil surface sealing, compaction and erosion  
33 (Bedaiwy 2008). This energy is directly related to drop diameter and velocity (Kincaid  
34 1996). In kinetic energy analyses of sprinkler irrigation, drop velocity was estimated  
35 using simulation models (Kincaid 1996). When it comes to simulating sprinkler  
36 irrigation, the distribution of drop diameters is a primary input. An adequate  
37 characterization of this variable is required to estimate the differences in performance  
38 resulting from different irrigation equipments, operating conditions or changes in the  
39 environment (particularly wind speed). Ballistic sprinkler simulation models (Carrión et  
40 al. 2001; Playán et al. 2006) require this information to estimate the landing point and  
41 terminal velocity of drops resulting from a certain irrigation event. Procedures have  
42 been developed to estimate drop diameter distribution at the nozzle from the sprinkler  
43 application pattern using inverse simulation techniques (Montero et al. 2001; Playán et  
44 al. 2006). Following these techniques, drop distributions can be identified that  
45 reproduce observed application patterns.

46 As a consequence of these irrigation management and simulation needs, irrigation drop  
47 characterization has been a traditional field of research. Different techniques have been  
48 developed since the end of the 19<sup>th</sup> Century (Wiesner 1895). The evolution of drop  
49 characterization techniques as related to natural or irrigation precipitation has been  
50 reported by a number of authors (Cruvinel et al. 1996; Cruvinel et al. 1999; Salles et al.  
51 1999; Sudheer and Panda 2000; Montero et al. 2003). A succinct discussion of the  
52 methods reported in these papers follows:

- 53 • **Stain method.** It is based on the measurement of the stain created by a drop when  
54 impacting on an absorbing surface. Since stain and drop diameters are correlated,  
55 stain diameters can be used to estimate drop diameters (Magarvey 1956).
- 56 • **Flour method.** Drops impacting on a thin layer of flour create pellets whose mass  
57 or diameter is statistically related to drop diameter (Kohl and DeBoer 1984)
- 58 • **Oil immersion method.** Based on the fact that water droplets can get trapped in a  
59 fluid with adequate density. Drops are then observed with appropriate optical  
60 equipment to measure their diameter (Eigel and Moore 1983)
- 61 • **Momentum method.** Includes a variety of techniques (mostly applied to natural  
62 precipitation) based on the use of pressure transducers to estimate the kinetic  
63 properties of sets of drops (Joss and Waldvogel 1967).
- 64 • **Photographic method.** The methodology is based on high-speed photographs of  
65 drops in an irrigation jet. The technique first focused on photographing raindrops  
66 (Jones 1956). Recently, photographs have been used to estimate drop diameter  
67 through digital techniques (Sudheer and Panda 2000).
- 68 • **Optical methods.** In the last decade of the 20<sup>th</sup> Century, two types of optical  
69 methods were applied to measure drop diameter. The first one is based on the  
70 analysis of the deviation of a laser flow as it passes through drops of different

71 characteristics (Kincaid et al. 1996). The second one, the optical disdrometer,  
72 measures the attenuation of a luminous flow (Hauser et al. 1984; Montero et al.  
73 2003). Both methods provide automated estimates of drop diameter in a set of drops.  
74 Optical methods count on the advantage of being fully automated in data collection,  
75 thus permitting fast, repeatable drop characterization. These methods have however  
76 specific sources of errors, such as those induced by side-passing drops and overlapping  
77 drops. Recently, (Burguete et al. 2007) presented a simulation study characterizing the  
78 relevance of these errors under a number of experimental conditions, and proposed a  
79 statistical method to reject erroneous drops. Burguete et al. (2007) theoretically  
80 analysed the use of the disdrometer to estimate drop velocity from drop time of passage,  
81 and found it subjected to large experimental errors.

82 The need for an alternative, simple method for evaluating the characteristics of sets of  
83 drops motivated the search for a direct drop characterization method able to provide  
84 information on at least drop diameter and velocity. Recent developments in digital  
85 photography oriented the search towards a photographic method which could be used to  
86 obtain data sets adequate for detail analysis of sprinkler irrigation problems. Such a  
87 method stands as an attractive alternative, since it does not require specific equipment.

88 In this paper a new photographic technique is presented, validated and tested. The  
89 technique permits to measure the diameter, velocity and angle (in a vertical plane  
90 containing the drop trajectory) of each drop. The proposed technique is based on low-  
91 speed photography rather than on high-speed photography. Under low-speed conditions,  
92 drops are photographed as traces of the drop trajectory, thus permitting determination of  
93 the three abovementioned variables. Under high-speed conditions, it is only possible to  
94 determine drop diameter, since drops are visualized as spheres. The results of the

95 proposed low-speed photography technique were applied in this paper to characterize  
96 water application resulting from an isolated impact sprinkler.

## 97 **MATERIALS AND METHODS**

### 98 **Basic experimental set up**

99 A VYR35 impact sprinkler (VYRSA, Burgos, Spain) was used in all experiments. This  
100 model is commonly used in solid-set systems in Spain. The sprinkler was equipped with  
101 a 4.8 mm nozzle (including a straightening vane). An isolated sprinkler was installed at  
102 an elevation of 2.15 m and operated at a nozzle pressure of 200 kPa. The sprinkler  
103 revolution time was 27.5 s. A volumetric water meter was used to estimate sprinkler  
104 discharge. The experimental runs were performed at the CITA farm located in  
105 Montañana, Zaragoza (Spain). A plot was chosen which was protected from the  
106 prevailing winds by a windbreak. Experiments were performed in periods of  
107 inappreciable wind.

### 108 **Characterization of the radial application pattern**

109 In order to achieve this objective, 28 pluviometers were installed on the experimental  
110 plot along a sprinkler radius, covering distances from 1.5 m to 14.0 m, with 0.5 m  
111 interval. The pluviometer dimensions were in compliance with the ISO 15886-3 norm.  
112 The irrigation test lasted for two hours, during which 2.495 m<sup>3</sup> of irrigation water were  
113 applied (average discharge of 0.347 L s<sup>-1</sup>).

### 114 **Preliminary photographic experiments for drop characterization**

115 Using a relatively low shutter speed, drops are represented in the photographs as  
116 cylinders, thus permitting the identification of drop diameter and length of run (by  
117 comparison with a photographed reference ruler), and vertical angle. Drop velocity can  
118 be derived from the length of run and the shutter speed.

119 Preliminary experiments were performed to identify optimum camera operation  
120 conditions for outdoor drop identification. The camera zoom was always set at 70 mm.  
121 After trying several background screen colours, black was chosen as the best option for

122 drop characterization. In a second step, different shutter speeds (100, 125 and 160) and  
123 diaphragm openings (from F4.5 to F29) were tested. The chosen combination was a  
124 shutter speed of 100 (1/100 s) and F11. These camera adjustments resulted in sharp drop  
125 cylinder images.

126 In all subsequent experiments, the camera and the screen were installed as depicted in  
127 Fig. 1, to allow for drops to fall between them. The screen was built to suit the needs of  
128 the experiment. It consisted of a plastic rectangle of 0.30 x 0.40 m covered with a black  
129 cloth to prevent drops on the plastic material from shining and thus disturbing the  
130 characterization of falling drops. A reflecting metallic lateral was mounted on the side  
131 of the screen (opposite to the sun) to increase the drop brightness by duplicating the  
132 source of light (sun and reflector). The screen was installed at a distance of 1.00 m from  
133 the camera objective. The reference ruler was installed on the screen, at a distance of  
134 0.25 m from it (0.75 m from the camera objective). The camera was manually focused  
135 on the reference ruler.

136 Subsequently, tests were performed to determine how many photographs could be taken  
137 when shooting in continuous mode and what the speed of picture taking was. These  
138 values depend of the selected photo quality. Quality "L" (3,872 by 2,592 pixels) was  
139 selected because this was the highest available image resolution in JPEG format, and  
140 the picture taking speed was adequate (2.9 photos per second). The combination of  
141 photo quality, zoom regulation and distance to the target resulted in a density of  
142 14-15 pixels  $\text{mm}^{-1}$ . As a consequence, drops of 0.5 mm would have a diameter of about  
143 7 pixels, while drops of 5 mm would have a diameter of 70-75 pixels. Regarding the  
144 length of the drop trace (cylinder height), it fluctuated between 130 and 1,050 pixels,  
145 depending on drop velocity.

## 146 **Validation of the proposed photographic method**

147 An experiment was performed to validate the main features of the method. Drops were  
148 modelled using metallic spheres of known diameter and physically determined velocity.  
149 A digital micrometer was used to determine an average diameter of 4.49 mm, and a  
150 coefficient of variation in diameter of 0.69 %. The experimental density of the lead-  
151 based spheres was  $11.2 \text{ Mg m}^{-3}$ . A set of spheres was released from an elevation of  
152 0.55 m over the 0 mark on the reference ruler. Photographs were used to determine  
153 sphere diameter and velocity. Due to the short trajectory of the spheres and the high  
154 metal density, acceleration was relevant when spheres were photographed.  
155 Consequently, for each sphere, the elevation from the release point to the centre of the  
156 photographed trajectory was determined. In order to test the photographic depth-of field  
157 and to estimate the related errors, spheres were released from five different points,  
158 differing in distance to the camera objective. The first release point was just above the  
159 reference ruler. The remaining four points were closer to the camera objective by 0.02,  
160 0.04, 0.06 and 0.08 m, respectively. In all five cases, the camera objective was focused  
161 to the reference ruler.

162 Diameter validation consisted on comparing micrometric measurements and  
163 photographic estimates of sphere diameter at different distances from the reference  
164 ruler. Regarding sphere velocity, the ballistic theory applied to drop movement was  
165 analysed (Fukui et al. 1980; Seginer et al. 1991). Under the experimental conditions the  
166 drag force was orders of magnitude smaller than the sphere weight. As a consequence,  
167 sphere movement could be approximated by the free fall equation:

$$168 \quad V = \sqrt{2 g h} \quad [1]$$

169 Where  $V$  is vertical velocity,  $g$  is the acceleration of gravity, and  $h$  is elevation from the  
170 release point.

171 **Experimental runs for drop characterization: field procedures**

172 Field experiments for drop characterization began at the experimental plot with the  
173 isolated sprinkler (Fig. 1), in sessions lasting between one and two hours. Nozzle  
174 pressure was controlled with a manometer and adjusted to 200 kPa. A radial line was  
175 marked on the soil extending from the sprinkler to the last observation point. The line  
176 was marked in every experimental period so that it formed a horizontal angle of about  
177 5° with the sun. Observation points for drop photography were marked on the line at  
178 distances of 1.5, 3.0, 4.5, 6.0, 7.5, 9.0, 10.5 and 12.5 m from the sprinkler. While the  
179 interval between observation points was usually 1.5 m, between the last two observation  
180 points the interval was 2.0 m. This interval was chosen so that photographs could be  
181 taken at 12.5 m, the last distance from the sprinkler at which drops could be appreciated  
182 at the camera elevation (0.80 m). It was judged interesting to photograph the drops  
183 reaching the largest distances from the sprinkler.

184 At each observation point, the camera and the screen were installed (Fig. 1). When the  
185 sprinkler jet approached the measurement line, the camera shooting was activated in  
186 continuous mode. Shooting stopped when drops could not be appreciated.  
187 Consequently, the number of photographs was different in each experimental run. In  
188 fact, this number depended on the time the jet stayed over the observation point (in turn  
189 dependent on distance to the sprinkler). This procedure was repeated between three and  
190 ten times at each observation point, depending on the local drop density (number of  
191 drops per unit photographed area). Drop density was very high near the sprinkler, while  
192 at the distal areas a large number of photographs were required to obtain a  
193 representative sample of the local drop population.

194 Although the sprinkler nozzle produces one compact jet of drops, the sprinkler impact  
195 arm takes some of its water to create a new, small jet at a certain horizontal angle. At

196 distances of 6.0 and 7.5 m from the sprinkler, the time lag between the drops coming  
197 from the impact arm and those coming from the main jet was long enough to  
198 photograph both sources of drops separately. At smaller distances no distinction could  
199 be made, while impact arm drops were not observed at distances exceeding 7.5 m.

#### 200 **Experimental runs for drop characterization: office procedures**

201 At every observation point a large number of photographs were taken. Some of them  
202 showed drops of adequate quality. These photographs were selected for further analysis  
203 using Microsoft Picture Manager®. The values of brightness, contrast and semitone  
204 were fixed at 60, 85 and 100 %, respectively, for all images.

205 The GIMP2© software (University of California, Berkeley, USA) was used for drop  
206 analysis. Drops adequately focused (located near the vertical plane containing the  
207 reference ruler) were numbered for future reference. Due to the available image  
208 resolution, drops not reaching 0.3 mm in diameter were discarded since it was  
209 impossible to assess if they were focused. The following step was to measure drop  
210 length, angle respect to the horizontal (setting the 0° at the line starting at the camera  
211 objective and perpendicularly intersecting the sprinkler riser), and drop diameter  
212 (correcting the number of horizontal pixels with the drop angle). If for a given drop the  
213 complete cylinder was not represented in the photograph, drop velocity was not  
214 measured. However, the drop diameter and angle were added to the drop database. All  
215 values were initially registered in pixels and transformed to mm using the pixel mm<sup>-1</sup>  
216 ratio obtained from the analysis of the image of the reference ruler. Histograms of the  
217 three analyzed variables were produced at each observation distance.

218 Drop diameter was combined with the sprinkler application pattern to estimate  
219 cumulative applied volume at a certain distance from the sprinkler.

## 220 **RESULTS AND DISCUSSION**

### 221 **Characterization of the radial application pattern**

222 The first step for sprinkler characterization was to obtain the radial application pattern  
223 using pluviometer data (Figure 2). The resulting pattern is characteristic of impact  
224 sprinklers operating at low pressure. It shows low precipitation values (as low as  
225  $1.2 \text{ mm h}^{-1}$ ) at intermediate distances (5-7 m from the sprinkler), and maximum values  
226 near the end of the irrigated area. The minimum recorded precipitation was  $0.2 \text{ mm h}^{-1}$   
227 at 14.0 m from the sprinkler, while the maximum precipitation was  $2.8 \text{ mm h}^{-1}$  at  
228 11.0 m. The average precipitation along the irrigated radius was  $1.6 \text{ mm h}^{-1}$ .

### 229 **Validation of the proposed photographic method**

230 Photographs taken at distances between the spheres and the vertical plane containing the  
231 reference ruler of 0.06 and 0.08 m were out of focus and could not be evaluated. As a  
232 consequence, the proposed method characterizes drops located in a range of  $\pm 0.04 \text{ m}$   
233 from the focus point (the reference ruler). A total of 43 photographs containing 138  
234 trajectories of the validation metallic spheres (corresponding to the distances to the  
235 reference ruler of 0.00, 0.02 and 0.04 m) were evaluated.

236 The average measured sphere diameters were 4.47, 4.59 and 4.60 mm, for distances of  
237 0.00, 0.02 and 0.04 m, with respective coefficients of variation of 2.01, 2.74 and  
238 3.13 %. The increase in diameter with decreased distance to the target reflects the error  
239 derived from spheres which appear larger than they are because they are closer to the  
240 camera objective. In the worst case, spheres with a real diameter of 4.49 mm resulted in  
241 estimated diameters of 4.60 mm. As a consequence, the proposed method results in a  
242 maximum average error of  $\pm 2.45 \%$  at a distance of 0.04 m from the reference ruler.  
243 Under a random fall of spheres, the errors produced on both sides of the reference ruler  
244 cancel, and the average error can be approximated by the average diameter error at a

245 distance of 0.00 m (-0.45 %). These maximum and average error figures are moderate,  
246 and can be compared to the manufacturing coefficient of variation of the spheres  
247 ( $\pm 0.69\%$ ).

248 Regarding drop velocity, the average simulated velocity was  $3.26 \text{ m s}^{-1}$ . The average  
249 measured velocities were 3.27, 3.28 and  $3.22 \text{ m s}^{-1}$  at 0.00, 0.02 and 0.04 m from the  
250 reference ruler, respectively. The expected average error corresponds to the error at  
251 0.00 m (0.31 %), while the maximum average error was 1.23 % at a distance of 0.04 m  
252 from the ruler. In the case of sphere velocity, however, photographic measurements  
253 were compared to simulation results, not to velocity measurements.

254 Drop angle was not validated, due to the physical nature of its measurement procedure  
255 and its independence from the distance to the reference ruler.

256 The errors in diameter and velocity resulting from the spheres being closer or further to  
257 the camera objective than the reference ruler cancel out when average values are  
258 produced. These errors result in modified distributions of diameters and velocities. The  
259 maximum errors have been bounded in the reported experiment ( $\pm 2.45\%$  for diameter  
260 and  $\pm 1.23\%$  for velocity). These error bounds must be taken into consideration when  
261 analysing the results presented in this paper, but the magnitude of the errors does not  
262 compromise the validity of the results.

### 263 **Basic drop statistics**

264 A large number of photographs (about 600) were taken. Only 184 of them contained  
265 valid drops. The rest of the photographs were taken before or after the jet passage, or  
266 contained very few, unfocused drops. The total number of valid drops was 1,464.  
267 Table 1 presents basic statistics (mean, minimum and maximum) of the number of  
268 drops and the analyzed variables (arithmetic diameter, volumetric diameter, velocity and  
269 angle) as a function of the distance to the sprinkler. The number of drops ranged from

270 61 at 12.5 m to 354 at 1.5 m. Average drop diameter increased with distance, with a  
271 minimum of 0.6 mm at 1.5 m, and a maximum of 3.3 mm at 12.5 m. The volumetric  
272 diameter followed a similar pattern, increasing from 0.7 mm at 1.5 m to 4.1 mm at  
273 12.5 m. Drop velocity also increased with distance, ranging from  $1.9 \text{ m s}^{-1}$  by the  
274 sprinkler to  $5.6 \text{ m s}^{-1}$  at the limit of irrigated area. Average angle values resulted quite  
275 variable, and it was not possible to appreciate a relationship with distance to the  
276 sprinkler. In the proximal region the angle was sometimes larger than  $90^\circ$ . This can be  
277 attributed to the fact that the experimental setup was located outdoor. As a consequence,  
278 turbulences could have distorted drop angle, particularly for small drop diameters. An  
279 extended version of Table 1, individualizing each drop within each distance from the  
280 sprinkler, can be downloaded from [www.eead.csic.es/drops](http://www.eead.csic.es/drops).

281 Figure 3 presents photographs of drops #204, #646 and #1,456. At the bottom of each  
282 picture, information is provided on the distance to the sprinkler (D), drop diameter ( $\varnothing$ ),  
283 drop velocity (V) and drop angle ( $\hat{\alpha}$ ). To ease visualization, images are presented in  
284 different scales. The photographs depict drops as transparent cylinders, and permit  
285 accurate, direct determination of their size, even for the smallest diameters. The quality  
286 of the photographs permits to obtain the information required to characterize the  
287 sprinkler application pattern at any distance. Comparison between the three pictures  
288 illustrates the effect of the distance to the sprinkler on drop diameter (increase) and  
289 velocity (increase).

### 290 **Drop diameter vs. distance**

291 Drop diameter distribution histograms are presented in Fig. 4 for all distances to the  
292 sprinkler. As the distance to sprinkler increases, the frequency of large drops increases.  
293 The smooth transition observed for distances up to 9.0 m becomes abrupt between  
294 distances of 9.0 and 10.5 m. These differences could be attributed to the fact that drops

295 landing at distances under 10.5 m from the sprinkler can either be emitted from the  
296 nozzle or separate from the jet along its trajectory. This fact could explain the presence  
297 of drops with diameters under 1 mm (about 40 % at 9.0 m), which completely disappear  
298 at a distance of 10.5 m. From 10.5 m on, all drops seem to result from the disintegration  
299 of the jet, and the modal diameters are in the interval 2-4 mm. This hypothesis was  
300 presented by Von Bernuth and Giley (1984) and Seginer et al. (1991). Montero et al.  
301 (2003) reported similar results when analyzing drop diameter measurements performed  
302 with an optical disdrometer. The uncertainties associated to disdrometer measurements,  
303 evidenced by Burguete et al. (2007) raised some concern about the quantitative  
304 importance of these small drops. Photographic data confirm the relevance of small  
305 drops at large distances from the sprinkler, and pose additional concerns about the  
306 adequacy of sprinkler irrigation ballistic theory, specifically about the hypothesis stating  
307 that all drops are created at the nozzle.

308 At distances from the sprinkler of 6.0 and 7.5 m, part of the drops were identified as  
309 being created by the oscillations of the impact arm, while the rest of the drops were  
310 attributed to the main jet. In Figs. 4, 5 and 6, the frequency of these drops is presented  
311 in black columns. Since impact arm and main jet drops were separated in the Figure, it  
312 could be observed that impact arm drops were larger than main jet drops at each  
313 distance.

314 Drops under 1 mm constituted the most frequent class for distances up to 7.5 m. The  
315 observation distance with the largest frequency of small drops was 1.5 m (98 %). From  
316 this distance on, the frequency of small drops decreased as the frequency of large drops  
317 increased. The largest diameters (larger than 4 mm) were only present at distances of  
318 10.5 and 12.5 m, and showed frequencies of about 15 %. At a distance of 12.5 m, drops

319 exceeding 5 mm in diameter were more frequent than at 10.5 m, the other distance  
320 where they were found.

### 321 **Drop velocity vs. distance**

322 Drop velocity resulted more variable than drop diameter for each considered distance.  
323 Figure 5 presents the frequency of drop velocity at the observation points. An increase  
324 of velocity with distance can be appreciated in the Figure, where three patterns can be  
325 observed: 1) Up to a distance of 6 m, velocities were low-medium (up to  $5 \text{ m s}^{-1}$ ). Low  
326 velocities ( $< 3.0 \text{ m s}^{-1}$ ) prevailed at 1.5 m and at 3.0 m, accommodating about 95 % of  
327 the drops in both cases. At distances 4.5 m and 6.0 m, a gradual increase of velocity  
328 with distance was evidenced; 2) Between 7.5 and 9.0 m, a nearly homogeneous  
329 distribution of velocity could be observed in the range  $0\text{-}6 \text{ m s}^{-1}$ ; 3) Finally, for  
330 distances 10.5 and 12.5 m, velocities were in the medium-high range ( $4\text{-}6 \text{ m s}^{-1}$ ). Drops  
331 emerging from the impact arm (depicted in black in Fig. 5) showed higher velocities  
332 than the rest of drops at the same distances. This can be attributed to the  
333 abovementioned differences in diameter.

### 334 **Drop angle vs. distance**

335 Drop angle showed the widest fluctuations among the three analyzed variables (Fig. 6).  
336 While wind speed was inappreciable during the experiments, turbulences seem to have  
337 occasionally influenced drop angle, particularly for the smallest drops. Angles slightly  
338 under  $90^\circ$  should be expected, as characteristic of drops reaching the soil surface with a  
339 certain component of velocity in the  $x$  direction. Although most drops show angles in  
340 the range  $65\text{-}95^\circ$ , the frequency of drops falling with angles in the  $>95^\circ$  range is relevant  
341 at some distances. The drop diameter pattern (particularly the frequency of small drops)  
342 can contribute to explain the variability in drop angle. For distances of 9.0 m and

343 beyond, drops with angles exceeding  $85^\circ$  were practically non-existent (1 % at 9.0 and  
344 10.5 m; 0 % at 12.5 m). Drops landing at these distances were comparatively large and  
345 therefore less likely to be affected by turbulences. Drops with angle  $>85^\circ$  had a  
346 frequency of 96 % at a distance of 1.5 m. This result can be related to the small drop  
347 diameter ( $< 1$  mm in 98% of the drops). Drops with angle  $>85^\circ$  also showed a large  
348 frequency at 7.5 m (67 %). In the remaining distances, this range of angles was  
349 symbolic. Drops with angle  $75-85^\circ$  appeared in very variable frequencies. Drop angles  
350  $<75^\circ$  prevailed at larger distances, with frequencies of 83% at 9.0 m, 75 % at 10.5 m and  
351 98 % at 12.5 m. In the remaining distances, frequencies fluctuated without a clear trend.  
352 Drops emerging from the impact arm had lower angles than the rest of the drops at the  
353 same distances, with the most frequent class being  $<65^\circ$ . While this can be partially  
354 attributed to their comparatively large diameter, the action of the arm seems to modify  
355 the vertical drop trajectory respect to drops of similar diameter resulting from the main  
356 jet.

### 357 **Cumulative drop frequency and volume**

358 Cumulative drop frequency and volume vs. drop diameter are presented in Fig. 7  
359 (subfigures 1 and 2, respectively). The graphs show one cumulative line for each  
360 observation distance to the sprinkler. Cumulative frequency lines approach 100 % at  
361 smaller drop diameters than cumulative volume. This indicates that although the  
362 number of large drops is low, their volume contribution is quite large. The cumulative  
363 lines corresponding to distances 10.5 and 12.5 m greatly differ from the rest of distances  
364 both in frequency and in volume. This can be attributed to the differences in the  
365 frequency of large drops (exceeding 3 mm) presented in Fig. 4. In the graph presenting  
366 cumulative volume (Fig. 7.2) curves for distances 6.0, 7.5 and 9.0 appear separated and

367 present less slope than the 1.5, 3.0 and 4.5 m curves. These groups of curves showed a  
368 more similar pattern in cumulative frequencies (Fig. 7.1).

369 The cumulative frequency graph shows that small drops (<2 mm of diameter) exceeded  
370 90% frequency for distances below 10.5 m, reaching 100 % frequency (and even  
371 volume) for distances up to 4.5 m. At medium-large distances the situation changed,  
372 particularly in volume. At 6.0, 7.5 and 9.0 m the cumulative volume for small drops was  
373 70 %, 50 % and 65 %, respectively. At the largest distances, 10.5 and at 12.5 m, the  
374 curves were less steep both in frequency and volume, indicating that the distribution of  
375 diameters was well graded. The volume of small drops (< 2 mm) was 1.5 % at 10.5 m  
376 and 0.7 % at 12.5 m.

377 The drop diameter range 2-5 mm was not important in terms of frequency at medium  
378 distances (4.5 to 9.0 m), averaging 5 %. However, this diameter range represented 40 %  
379 of the applied volume. Similar findings could be reported for large drops (>5 mm in  
380 diameter) at 10.5 and 12.5 m, since these drops only represented 3 % in frequency but  
381 16 % in volume. Although frequency data are particularly interesting to analyze the  
382 validity of the ballistic model, the analysis of cumulative volume produces more insight  
383 on the significance of different drop diameter classes.

#### 384 **Relationships between drop diameter, velocity and angle**

385 In the previous paragraphs relationships were described between drop diameter and the  
386 other measured variables at each observation distance (Figs. 4, 5 and 6). These  
387 descriptions were qualitative, since the variables were grouped in diameter ranges and  
388 separated by distance to the sprinkler. Figures 8 and 9 present scatter plots between drop  
389 diameter on one hand and velocity and angle on the other, for all characterized drops.

390 A clear trend was observed between diameter and velocity (Fig. 8), which was  
391 represented by a logarithmic model ( $R^2 = 0.91$ ). This trend represents a varying

392 proportionality. The continuous decrease in slope is related to the relationship between  
393 drop diameter and aerodynamic drag, and to the fact that small drops are observed in  
394 their final, quasi vertical trajectory, while larger drops are usually observed when their  
395 trajectory still has a relevant horizontal component. Symbols in Fig. 8 represent the  
396 observation distance, and reveal that large drops are indeed observed at distal points,  
397 while finer drops can be observed at any point, but more frequently near the nozzle.

398 Figure 9 presents the relationship between drop diameter and drop angle. The Figure  
399 shows an important variability in angle for small drop diameters. The trajectory of small  
400 drops was occasionally affected by turbulences distorting their vertical angle.  
401 Variability sharply decreased with drop diameter. A significant linear relationship  
402 ( $p < 0.001$ ) could be established between both variables, although the coefficient of  
403 determination was very low. The application of the linear model to the estimation of  
404 drop angle for diameters of 0.5 and 5.0 mm resulted in angles of  $80.1^\circ$  and  $59.1^\circ$ ,  
405 respectively. As a consequence, a range of  $20^\circ$  in drop angle should be observed in the  
406 absence of turbulences in all drop diameters and for all observation points, with the  
407 most vertical trajectories corresponding to small drops.

#### 408 **Volumetric analysis of drop diameter and velocity**

409 Figure 10 presents the cumulative volume applied by each drop diameter class as a  
410 function of distance. An increase in the slope of cumulative volume lines was observed  
411 as drop diameter increased. This suggests that large drops contribute to sprinkler  
412 irrigation in a comparatively narrow circular crown. On the contrary, small drops  
413 contribute to the irrigation of wide circular crowns. 80 % of the volume applied by  
414 drops with diameter  $< 1$  mm fell between 0 and 6.0 m from the sprinkler, while 100 %  
415 fell between 0 and 9.0 m. At this last distance, drops with diameter of 1-2 mm had also  
416 applied practically all their volume. On the other hand, drops with diameter ranges 2-3

417 mm and 3-4 mm applied 63 % and 86 % (respectively) of their volume between 9.0 and  
418 12.5 m to the sprinkler. Between these two distances, the largest drop class (> 4 mm)  
419 applied 100 % of their volume.

420 Figure 11 presents a visual representation of the results reported in Fig. 10. Drops of  
421 different diameters are depicted and located in circular crowns centred at the  
422 observation points. In this quarter-circle representation, a sample of 500 drops (and half  
423 drops) are presented and located in each circular crown following the observed  
424 frequencies. The data included in the Figure present the drop distribution in the total  
425 area irrigated by the sprinkler in terms of drop frequency and associated volume.  
426 Confirming previous results, drop density drastically decreases with distance. At the  
427 same time, drop diameter increases and compensates (in terms of volume) the decrease  
428 in density. It is interesting to note that 71.6 % of the total drops had diameters <1 mm,  
429 with a volumetric contribution of just 7.9 %. On the other hand, the largest drops  
430 (>4 mm) had a frequency of 0.7 %, but their volumetric contribution was 27.1 %.

431 Finally, Figure 12 presents the arithmetic (Table 1) and volume weighed average drop  
432 velocity as a function of distance to the sprinkler. The volumetric average shows an  
433 approximately linear relationship between 2 and 6 m s<sup>-1</sup>, while the arithmetic average  
434 reports on a sharp increase in drop velocity between 9.0 and 10.5 m from the sprinkler.

#### 435 **Evaluation of the proposed photographic methodology**

436 The proposed method permits direct, visual measurement of the drop variables. It  
437 produces quality measurements of the photographed drop population. Photographic data  
438 quality is based on the individualization of the drops and on the physical nature of the  
439 geometric determinations. Additionally, the proposed technique is low-cost, easy to  
440 setup and transport (just a camera and a screen), does not require computing power in  
441 the field and permits to measure drop angles. Finally, the proposed technique obtains

442 three variables per drop, as compared to the diameter measurements reported in the  
443 literature for optical methods (Kincaid 1996; Montero et al. 2003).

444 Unfortunately, the method requires skilful operation in the field and time-consuming  
445 processing at the office. About 200 h of work were required to run the field and office  
446 phases of the reported experiments. Most of the time (about 7 min drop<sup>-1</sup>) was devoted  
447 to the estimation of drop variables from the treated images. As a consequence, the  
448 proposed method results cumbersome and time consuming. Automation of this process  
449 could be addressed using image processing, although the initial programming effort  
450 could be much more intense than the reported experimentation effort.

## 451 **CONCLUSIONS**

452 The proposed technique has permitted to estimate drop diameter, velocity and angle  
453 through direct measurements, thus guaranteeing quality in the characterization of the  
454 drops present in the photographs. The photographic technique is free from some of the  
455 problems that have been described for optical methods. Diameter and velocity  
456 measurements were successfully validated, with average errors of -0.45 and 0.31 %,   
457 respectively. A certain increase in the variability of diameter and velocity was  
458 appreciated, resulting from experimental errors and from the measurement of drops  
459 located at distances up to  $\pm 0.04$  m from the focus point. The proposed technique is  
460 cumbersome, just like many other direct measurement techniques reported in the  
461 literature (Sudheer and Panda 2000).

462 In the experimental case, results confirmed the differences in diameter, velocity and  
463 angle resulting from the distance to the sprinkler. The method permitted independent  
464 characterization of the drops emitted by the impact arm at distances of 6.0 and 7.5 m,  
465 showing relevant differences in the analysed variables with the main jet drops at the  
466 same distances. Very fine drops (<1 mm) were observed at distances of up to 9.0 m

467 from the sprinkler, a distance where their presence can not be explained by sprinkler  
468 irrigation ballistics (Lorenzini 2004). Our findings confirm similar results by Seginer et  
469 al. (1991), Montero et al. (2003) and Burguete et al. (2007), and stress the need to  
470 reformulate ballistic theory in the sense that not all drops are formed at the nozzle. The  
471 distribution of drop velocity followed the trends reported for drop diameter, while the  
472 angle showed high variability at some distances (particularly for fine drops), which was  
473 attributed to turbulences. The volumetric frequency of drop diameters permitted to  
474 reconstruct water application along the sprinkler radius in terms of the frequency of  
475 drops of different diameters.

476 The reported experiment was performed at a nozzle pressure of 200 kPa, which is  
477 substantially lower than the usual nozzle pressures for this type of impact sprinklers  
478 (300-400 kPa). Finer drops should be expected at these operating pressures, which  
479 could require specific adaptations of the proposed methodology.

480 The proposed technique does not require specific equipment, but it is labour intensive.  
481 This methodology can provide data to run drop-by-drop simulations aiming at  
482 improving the hypotheses behind ballistic models, particularly those addressing the  
483 process of drop formation along the jet. The reported drop velocity and angle  
484 measurements will be an additional source of validation for such simulation results.

485 **ACKNOWLEDGEMENTS**

486 This research was funded by the Plan Nacional de I+D+i of the Government of Spain,  
487 through grant AGL2007-66716-C03. Carlos Bautista received a scholarship from the  
488 Agencia Española de Cooperación Internacional (AECI). Thanks are also due to the  
489 Universidad Autónoma de Zacatecas, México. We appreciate the technical support  
490 provided by Valero Pérez, Miguel Izquierdo and Jesús Gaudó. The order of authors in  
491 the paper follows the “first-last-author-emphasis” norm.

492 **REFERENCES**

- 493 Bedaiwy MNA (2008) Mechanical and hydraulic resistance relations in crust-topped  
494 soils. *Catena* 72(2): 270-281.
- 495 Burguete J, Playán E, Montero J and Zapata N (2007) Improving drop size and velocity  
496 estimates of an optical disdrometer: Implications for sprinkler irrigation  
497 simulation. *Transactions of the American Society of Agricultural and Biological*  
498 *Engineers*, 50(6), 2103-2116.
- 499 Carrión P, Tarjuelo JM, and Montero J (2001) SIRIAS: a simulation model for sprinkler  
500 irrigation: I. Description of the model. *Irrigation Science*, 2001(20), 73-84.
- 501 Cruvinel PE, Minatel ER, Mucheroni ML, Vieira SR and Crestana S (1996) An  
502 Automatic Method Based on Image Processing for Measurements of Drop Size  
503 Distribution from Agricultural Sprinklers. *Anais do IX SIBIGRAPI*, 39-46.
- 504 Cruvinel PE, Vieira SR, Crestana S, Minatel R, Mucheroni ML and Neto AT (1999)  
505 Image processing in automated measurements of raindrop size and distribution.  
506 *Computers and Electronics in Agriculture*, 23(3), 205-217.
- 507 De Lima JLMP and Torf PJF (1994) Effects of wind on simulated rainfall and overland  
508 flow under single full-cone nozzle sprays. *Proceedings of the Second European*  
509 *Conference on Advances in Water Resources Technology and Management*. pp.  
510 443–450, In: Trakiris, G. and Santos, M.A., Editors,, Balkema, Lisbon, Portugal.
- 511 De Lima JLMP, Torfs PJF and Singh VP (2002) A mathematical model for evaluating  
512 the effect of wind on downward-spraying rainfall simulators. *Catena*, 46(4), 221-  
513 241.
- 514 Edling RJ (1985) Kinetic energy, evaporation and wind drift of droplets from low  
515 pressure irrigation nozzles. *Transactions of the American Society of Agricultural*  
516 *Engineers* 28(5): 1543-1550.

517 Eigel JD and ID Moore (1983) A simplified technique for measuring raindrop size and  
518 distribution. Transactions of the American Society of Agricultural Engineers  
519 26(4): 1079-1084.

520 Fukui Y, Nakanishi K and Okamura S (1980) Computer evaluation of sprinkler  
521 irrigation uniformity. Irrigation Science, 2, 23-32.

522 Hauser D, Amayenc P, Nutten B and Waldteufel P (1984) A new optical instrument for  
523 simultaneous measurement of raindrop diameter and fall speed distributions.  
524 Journal of Atmospheric and Oceanic Technology, 1(3), 256-269.

525 Jones DMA (1956) Rainfall drop-size distribution and radar reflectivity. Rainfall Drop-  
526 size. Distribution and Radar Reflectivity: 20.

527 Joss J and Waldvogel A (1967) Ein Spectrograph für Niederschlagstropfen mit  
528 automatischer Auswertung (A spectrograph for the automatic analysis of  
529 raindrops). Pure and Applied Geophysics. 68: 240–246.

530 Keller J and Bliesner RD (1990) Sprinkle and trickle irrigation. New York, NY, Van  
531 Nostrand Reinhold.

532 Kincaid DC (1996) Spraydrop kinetic energy from irrigation sprinklers. Transactions of  
533 the American Society of Agricultural Engineers 39(3): 847-853.

534 Kincaid DC, Solomon KH and Oliphant JC (1996) Drop size distributions for irrigation  
535 sprinklers. Transactions of the American Society of Agricultural Engineers,  
536 39(3), 839-845.

537 Kohl RA and DeBoer DW (1984) Drop size distributions for a low pressure spray type  
538 agricultural sprinkler. Transactions of the American Society of Agricultural  
539 Engineers 27(6): 1836-1840.

540 Lorenzini G (2004) Simplified modelling of sprinkler droplet dynamics. Biosystems  
541 Engineering 87(1): 1-11.

542 Lorenzini G (2006) Water droplet dynamics and evaporation in an irrigation spray.  
543 Transactions of the ASABE, 49(2), 545-549.

544 Magarvey RH (1956) Stain Method of drop size determination. Journal of Meteorology  
545 14: 182-184.

546 Montero J, Tarjuelo JM and Carrión P (2001) SIRIAS: a simulation model for sprinkler  
547 irrigation: II. Calibration and validation of the model. Irrigation Science,  
548 2001(20), 85-98.

549 Montero J, Tarjuelo JM and Carrión P (2003) Sprinkler droplet size distribution  
550 measured with an optical spectropluviometer. Irrigation Science, 2003(22), 47-  
551 56.

552 Playán E, Salvador R, Faci JM, Zapata N, Martínez-Cob A and Sánchez I (2005) Day  
553 and night wind drift and evaporation losses in sprinkler solid-sets and moving  
554 laterals. Agricultural Water Management, 76(3), 139-159.

555 Playán E, Zapata N, Faci JM, Tolosa D, Lacueva JL, Pelegrín J, Salvador R, Sánchez, I  
556 and Lafita A (2006) Assessing sprinkler irrigation uniformity using a ballistic  
557 simulation model." Agricultural Water Management, 84(1-2), 89-100.

558 Salles C, Poesen J and Borselli L (1999) Measurement of simulated drop size  
559 distribution with an optical spectro-pluviometer: Sample size considerations.  
560 Earth Surface Processes and Landforms, 24(6), 545-556.

561 Seginer I, Nir D and von Bernuth D (1991) Simulation of wind-distorted sprinkler  
562 patterns. Journal of Irrigation and Drainage Engineering, ASCE, 117(2), 285-  
563 306.

564 Sudheer KP and Panda RK (2000). Digital image processing for determining drop sizes  
565 from irrigation spray nozzles. Agricultural Water Management 45(2000): 159-  
566 167.

- 567 Tarjuelo, JM, Ortega JF, Montero J and De Juan JA (2000) Modelling evaporation and  
568 drift losses in irrigation with medium size impact sprinklers under semi-arid  
569 conditions. *Agricultural Water Management*, 43(2000), 263-284.
- 570 Thompson AL, Gilley JR and Norman JM (1986) Simulation of sprinkler water droplet  
571 evaporation above a plant canopy. Paper - American Society of Agricultural  
572 Engineers.
- 573 Trimer WL (1987) Sprinkler evaporation loss equation. *Journal of Irrigation and*  
574 *Drainage Engineering*, ASCE 113(4): 616-620.
- 575 Von Bernuth RD and Gilley JR (1984) Sprinkler droplet size distribution estimation  
576 from single leg test data. *Transactions of the American Society of Agricultural*  
577 *Engineers*, 27(5), 1435-1441.
- 578 Wiesner J (1895) Beiträge zur Kenntniss der Grösze des tropischen Regens. Akademie  
579 der Wissenschaften, Mathematika-Naturwissenschaften Klasse, vol. 104, Sitz  
580 Berlin Verlag, pp. 1397–1434.

581 **LIST OF TABLES**

582 Table 1. Basic statistics of the number of drops and analyzed variables for each distance

583 to the sprinkler.

584 **LIST OF FIGURES**

585 Figure 1: Experimental setup for drop characterization.

586 Figure 2: Radial application pattern for a VYR35 sprinkler equipped with a 4.8 mm  
587 nozzle (including a straightening vane) and operating at a pressure of 200 kPa.

588 Figure 3: Typical drop photographs, representative of three drop sizes. The information  
589 obtained from drops #204, #646 and #1,456 is presented in the figure ( $D$  = Distance  
590 to the sprinkler;  $\varnothing$  = Drop diameter ;  $V$  = Drop velocity; and  $\hat{\alpha}$  = Drop angle). A  
591 scale bar is presented within each picture.

592 Figure 4: Frequency of drop diameter classes at the observation points (distances of 1.5,  
593 3.0, 4.5, 6.0, 7.5, 9.0, 10.5 and 12.5 m from the sprinkler). Grey areas represent drops  
594 emitted from the main jet, while black areas represent drops emitted by the impact  
595 arm.

596 Figure 5: Frequency of drop velocity classes at the observation points (distances of 1.5,  
597 3.0, 4.5, 6.0, 7.5, 9.0, 10.5 and 12.5 m from the sprinkler). Grey areas represent drops  
598 emitted from the main jet, while black areas represent drops emitted by the impact  
599 arm.

600 Figure 6: Frequency of drop angle classes at the observation points (distances 1.5, 3.0,  
601 4.5, 6.0, 7.5, 9.0, 10.5 and 12.5 m). Grey areas represent drops emitted from the main  
602 jet, while black areas represent drops emitted by the impact arm.

603 Figure 7: Curves of cumulative drop frequency (1) and application volume (2).

604 Figure 8: Relationship between drop diameter and drop velocity. Each observation  
605 distance was represented with a different symbol.

606 Figure 9: Relationship between drop diameter and drop angle. Each observation  
607 distance was represented with a different symbol.

608 Figure 10. Cumulative volume applied by each drop diameter class as a function of  
609 distance to the nozzle. Data are presented for different drop diameter classes.

610 Figure 11. Representation of drop distribution resulting from the experimental sprinkler  
611 in a quarter-circle. A total of 500 drops (and half drops) are distributed at different  
612 distances from the nozzle.

613 Figure 12. Arithmetic and volume weighed average drop velocity as a function of  
614 distance to the sprinkler.

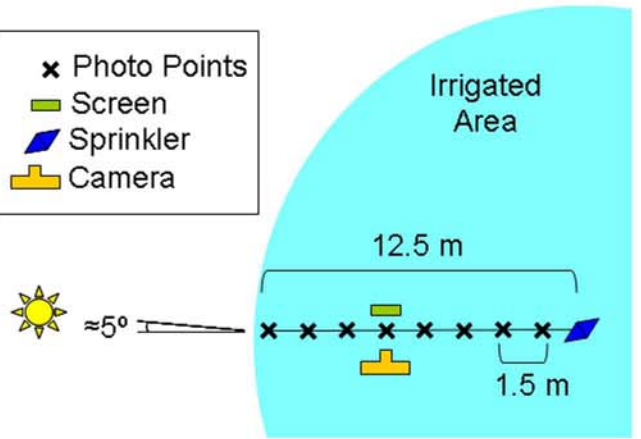
Table 1

<i>Distance (m)</i>	<i>Number of Drops</i>	<i>Diameter (mm)</i>			<i>Velocity (m s<sup>-1</sup>)</i>			<i>Angle (°)</i>		
		<i>Average</i>	<i>Min</i>	<i>Max</i>	<i>Average</i>	<i>Min</i>	<i>Max</i>	<i>Average</i>	<i>Min</i>	<i>Max</i>
<b>1.5</b>	354	0.6	0.4	1.6	1.9	1.0	3.8	94	65	105
<b>3.0</b>	205	0.7	0.5	1.6	2.4	1.4	3.6	70	53	84
<b>4.5</b>	135	0.8	0.3	1.8	2.5	0.9	4.1	75	39	112
<b>6.0</b>	260	0.9	0.4	2.5	2.5	0.9	5.2	67	43	98
<b>7.5</b>	156	1.1	0.4	3.8	3.1	0.9	5.9	88	60	107
<b>9.0</b>	184	1.1	0.4	3.1	3.3	1.0	6.3	67	51	86
<b>10.5</b>	109	3.0	1.3	6.8	5.6	4.2	7.5	73	61	87
<b>12.5</b>	61	3.3	1.7	6.4	5.5	4.2	7.2	69	60	79

Fig. 1

### PLAN VIEW

- × Photo Points
- Screen
- ▀ Sprinkler
- Camera



### EXPERIMENTAL SETUP

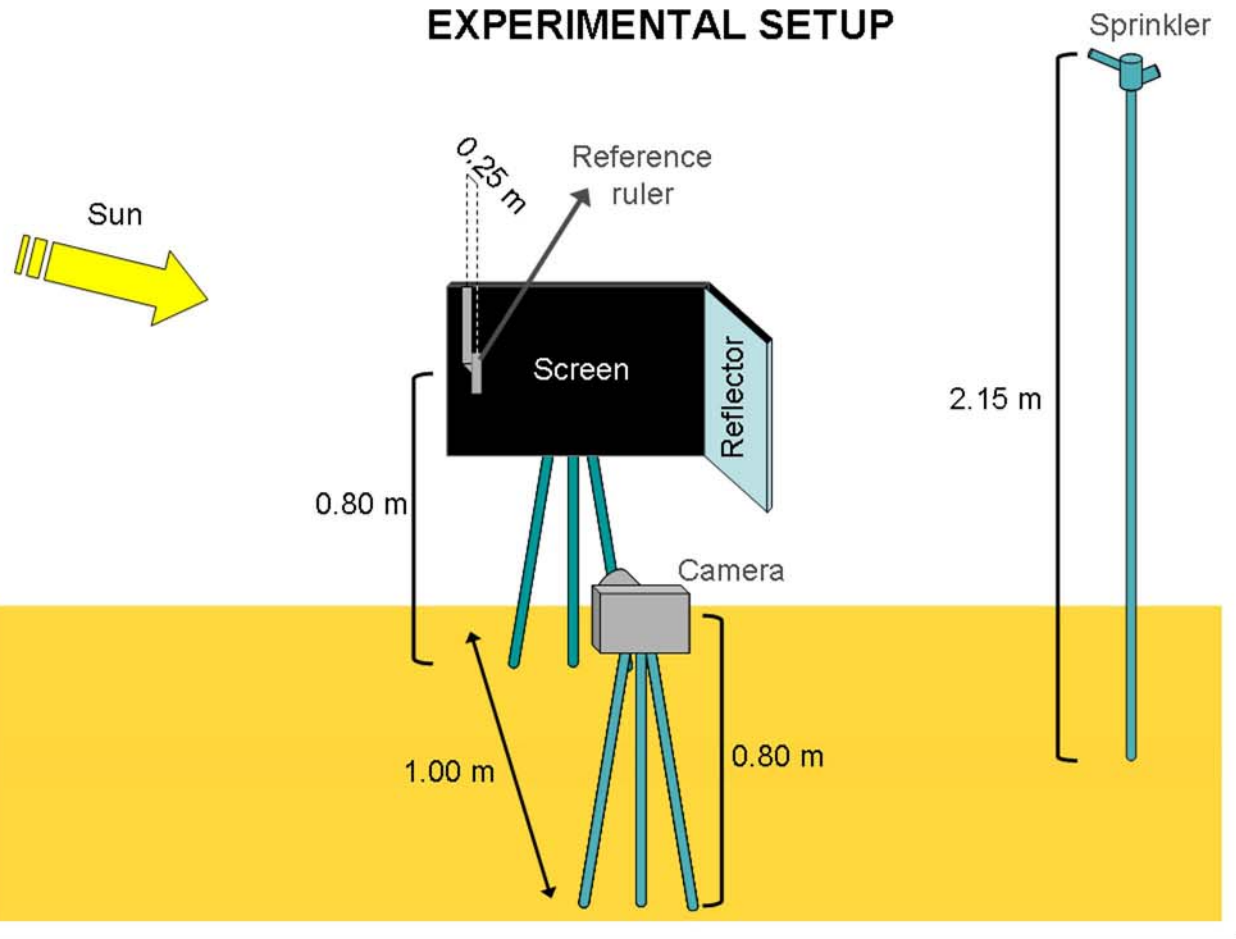


Fig. 2

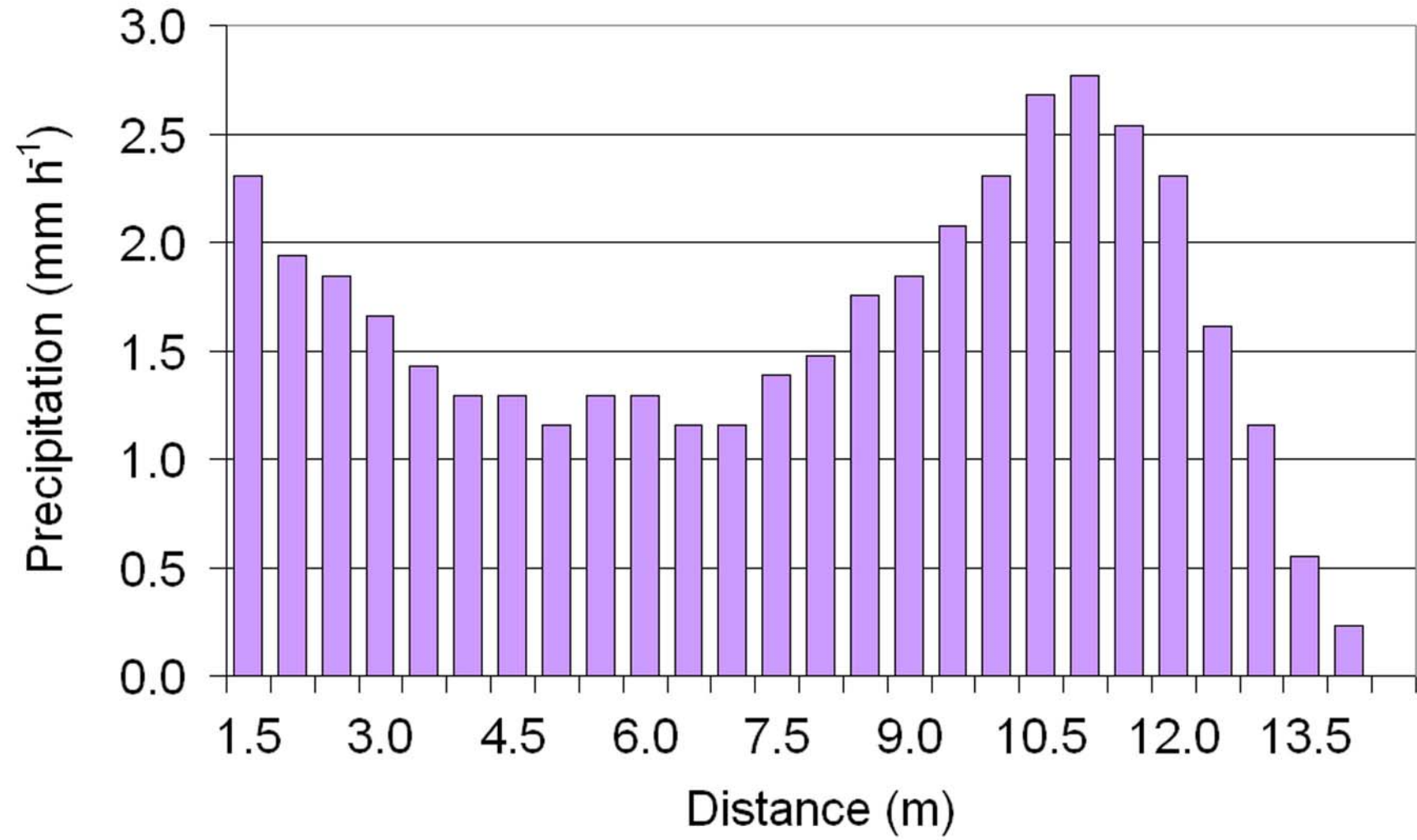
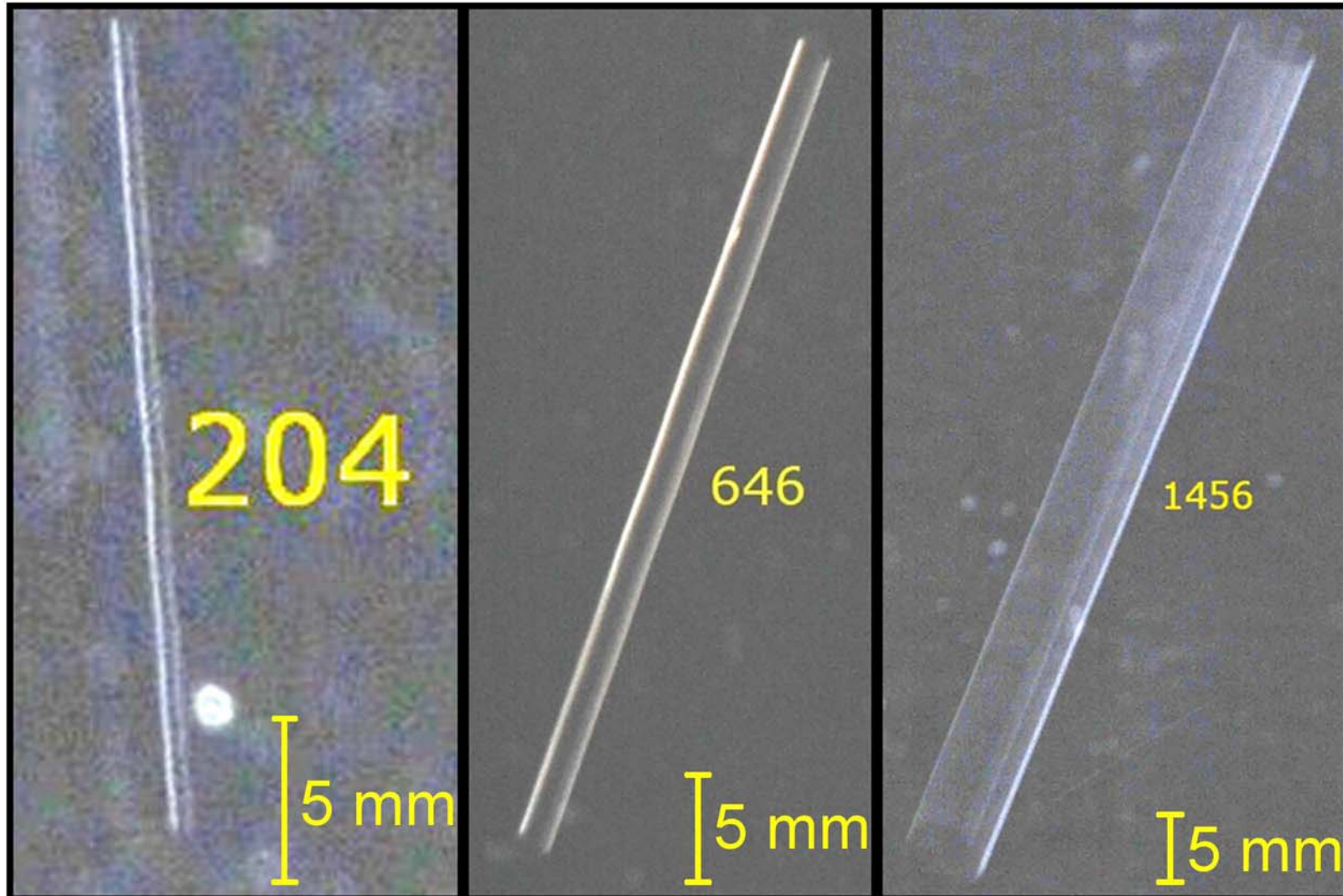


Fig. 3



**D = 1.5 m**  
 **$\varnothing = 0.66$  mm**  
**V = 1.9 m/s**  
 **$\hat{a} = 94^\circ$**

**D = 4.5 m**  
 **$\varnothing = 1.84$  mm**  
**V = 4.1 m/s**  
 **$\hat{a} = 71^\circ$**

**D = 12.5 m**  
 **$\varnothing = 6.36$  mm**  
**V = 6.4 m/s**  
 **$\hat{a} = 68^\circ$**

Fig. 4

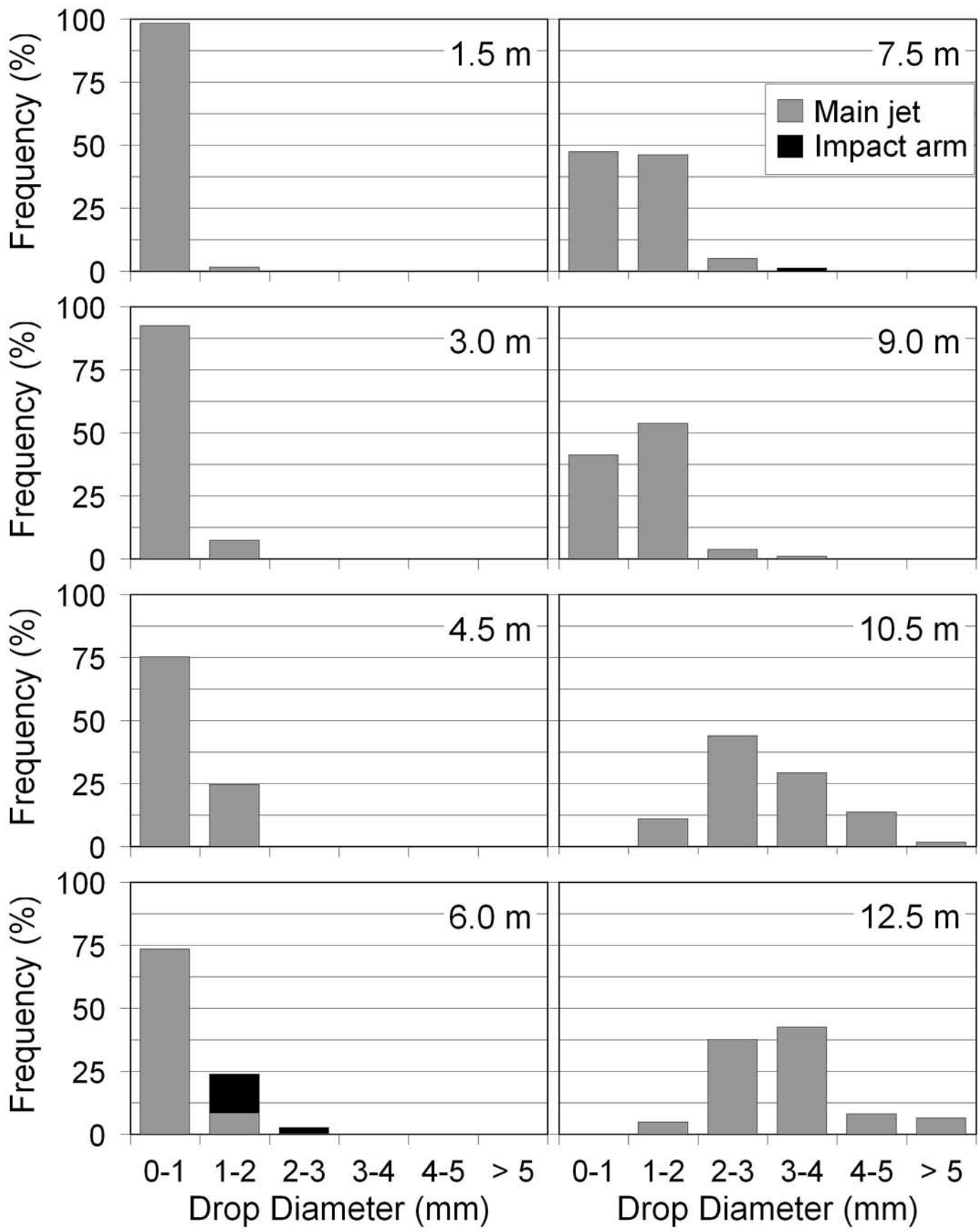


Fig. 5

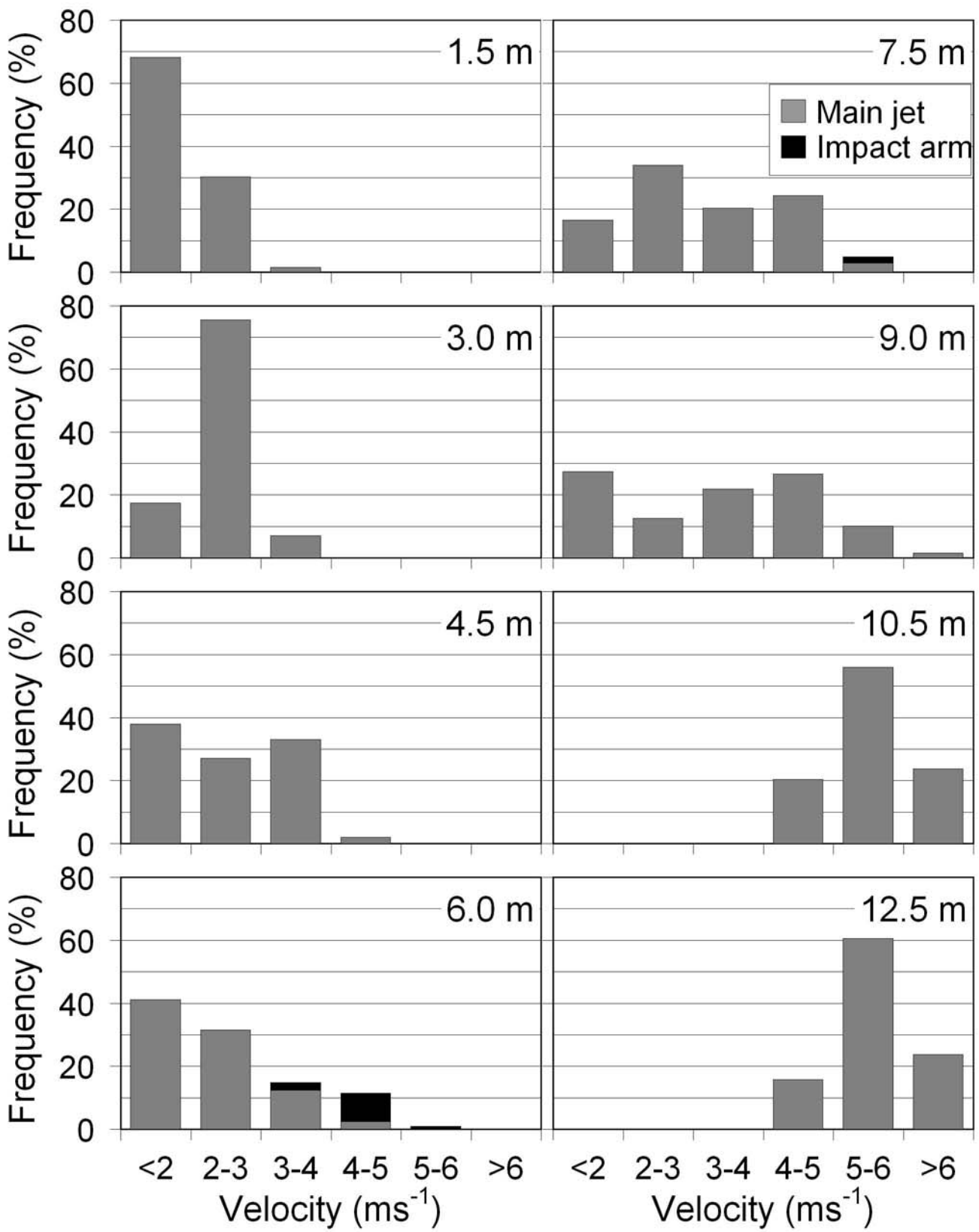


Fig. 6

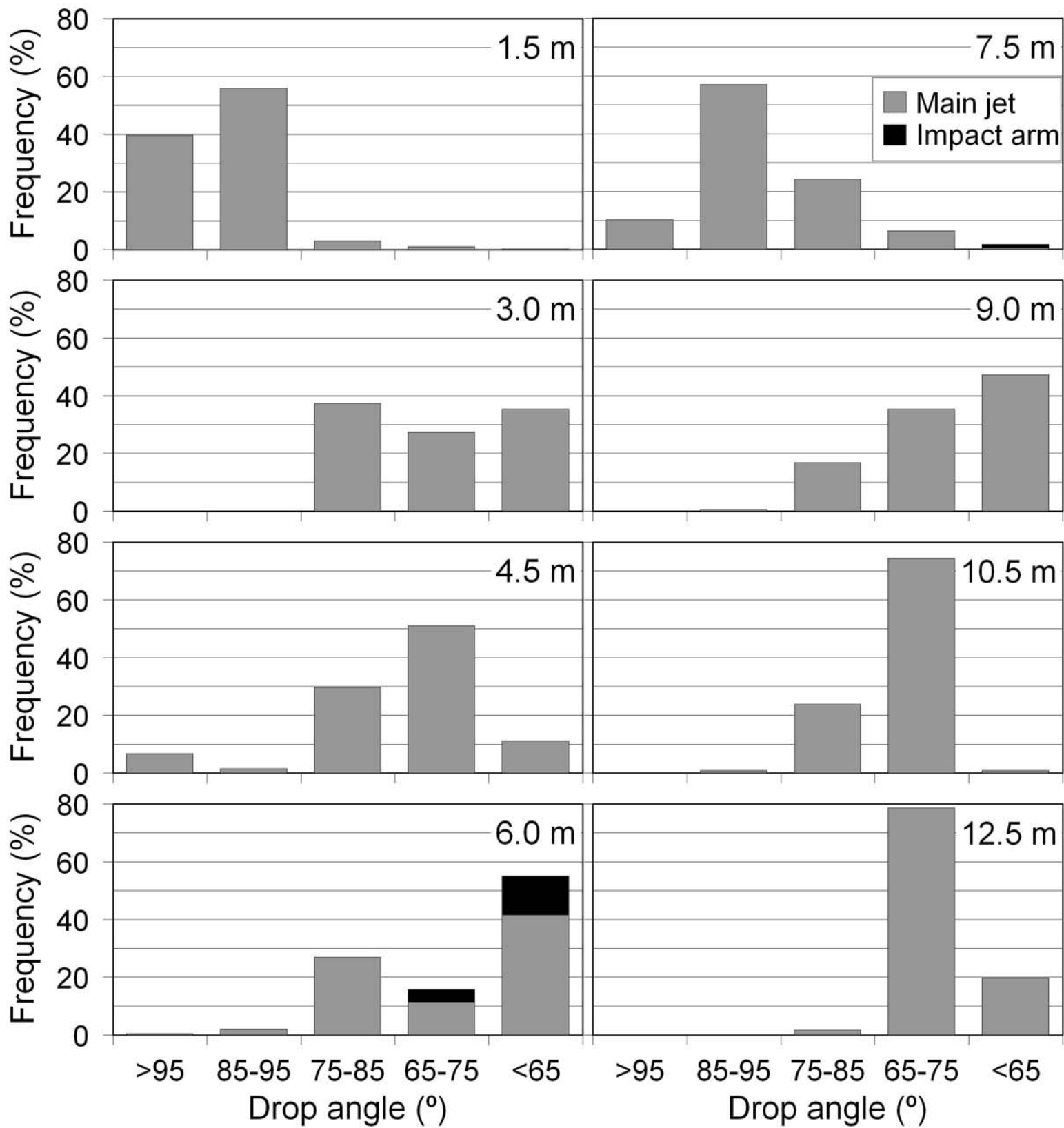


Fig. 7

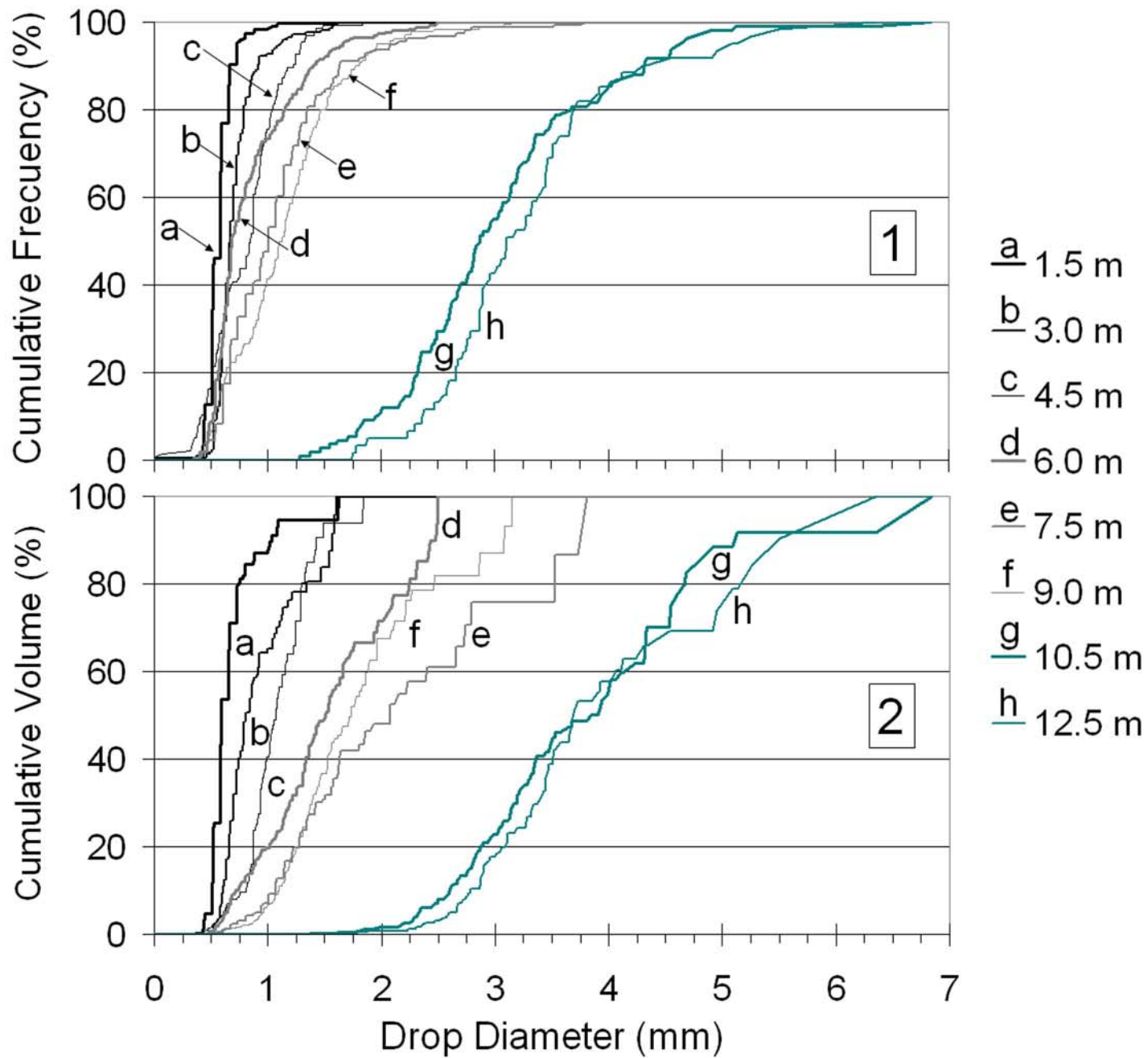


Fig. 8

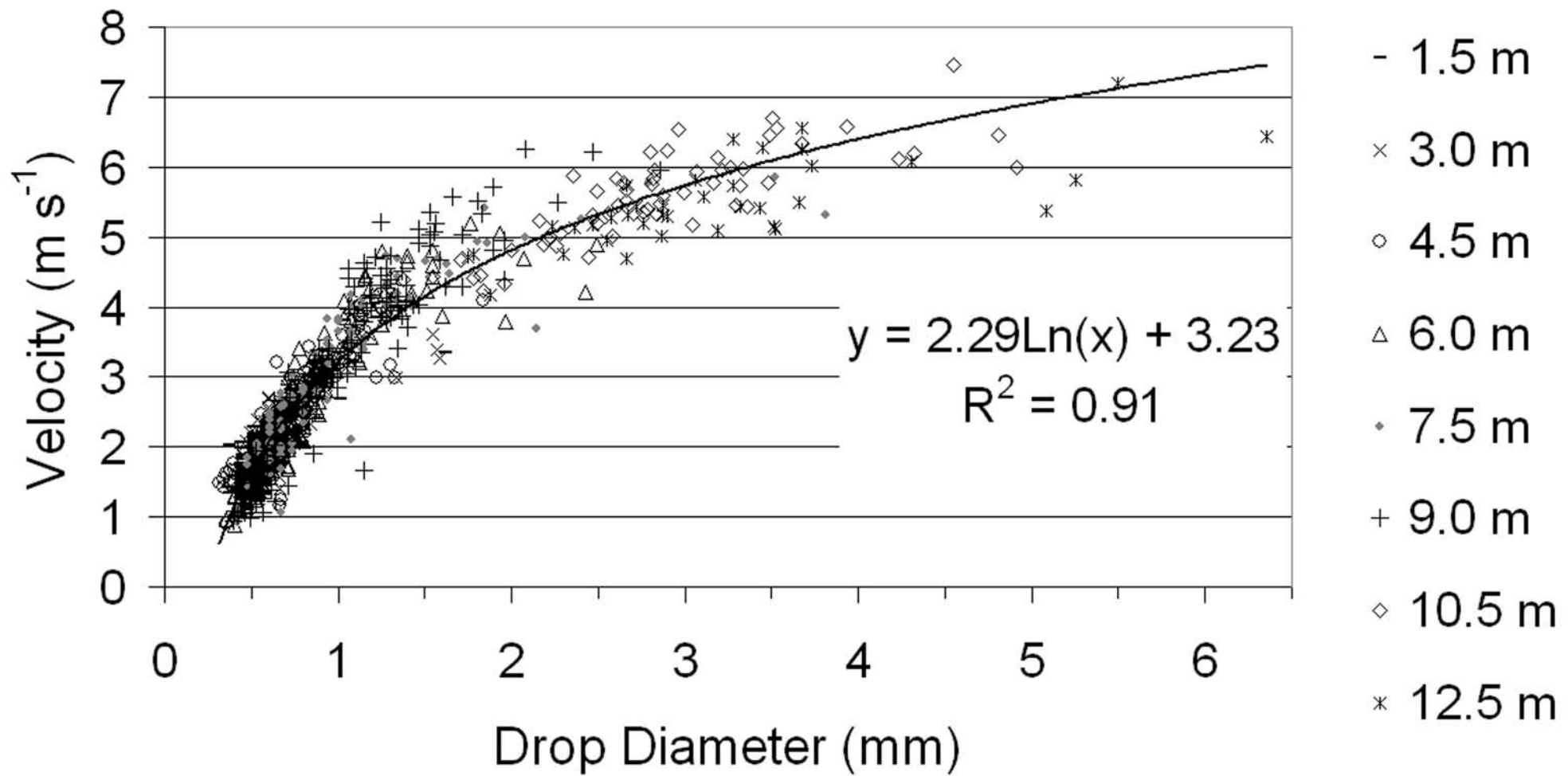


Fig. 9

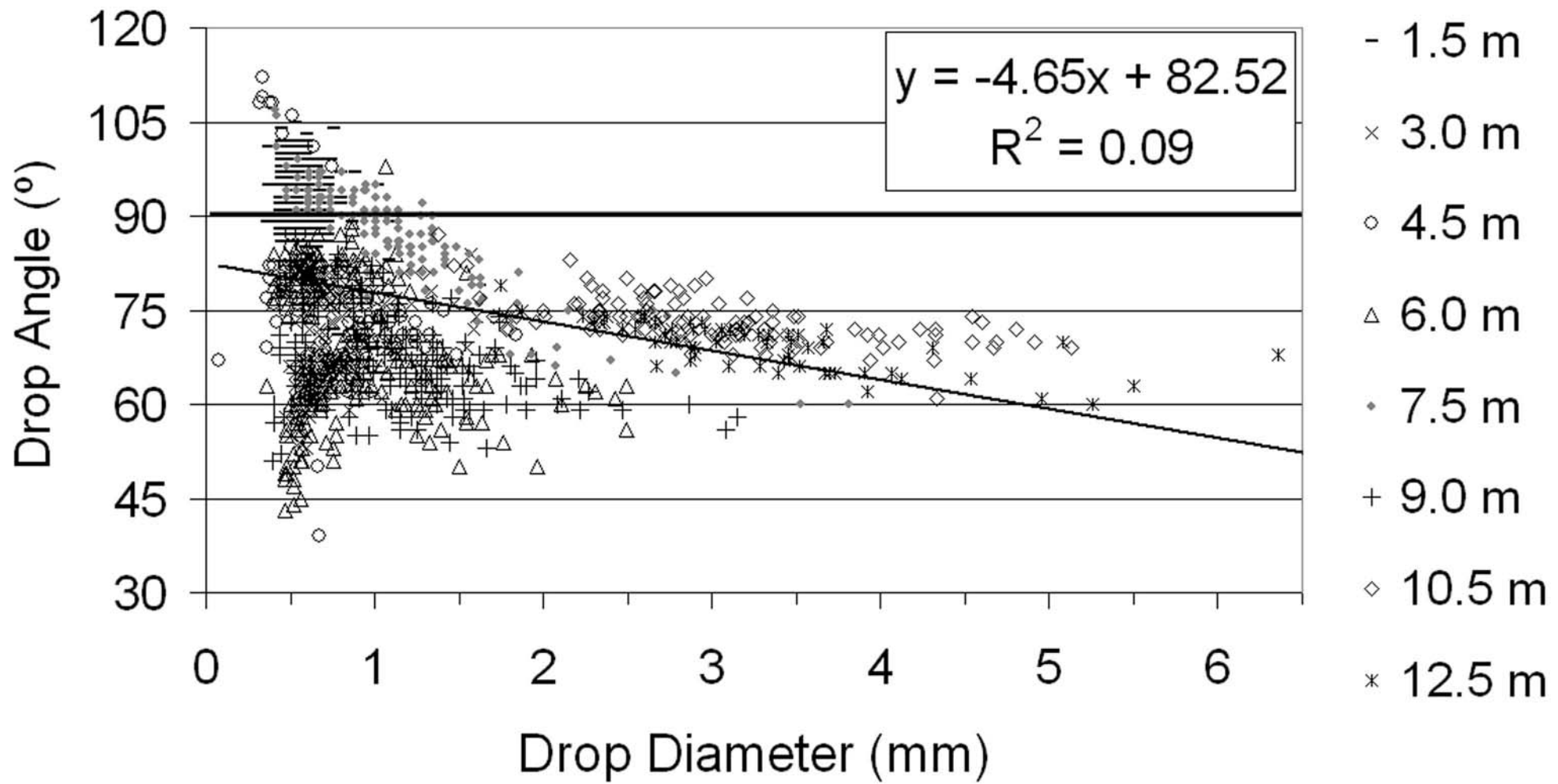


Fig. 10

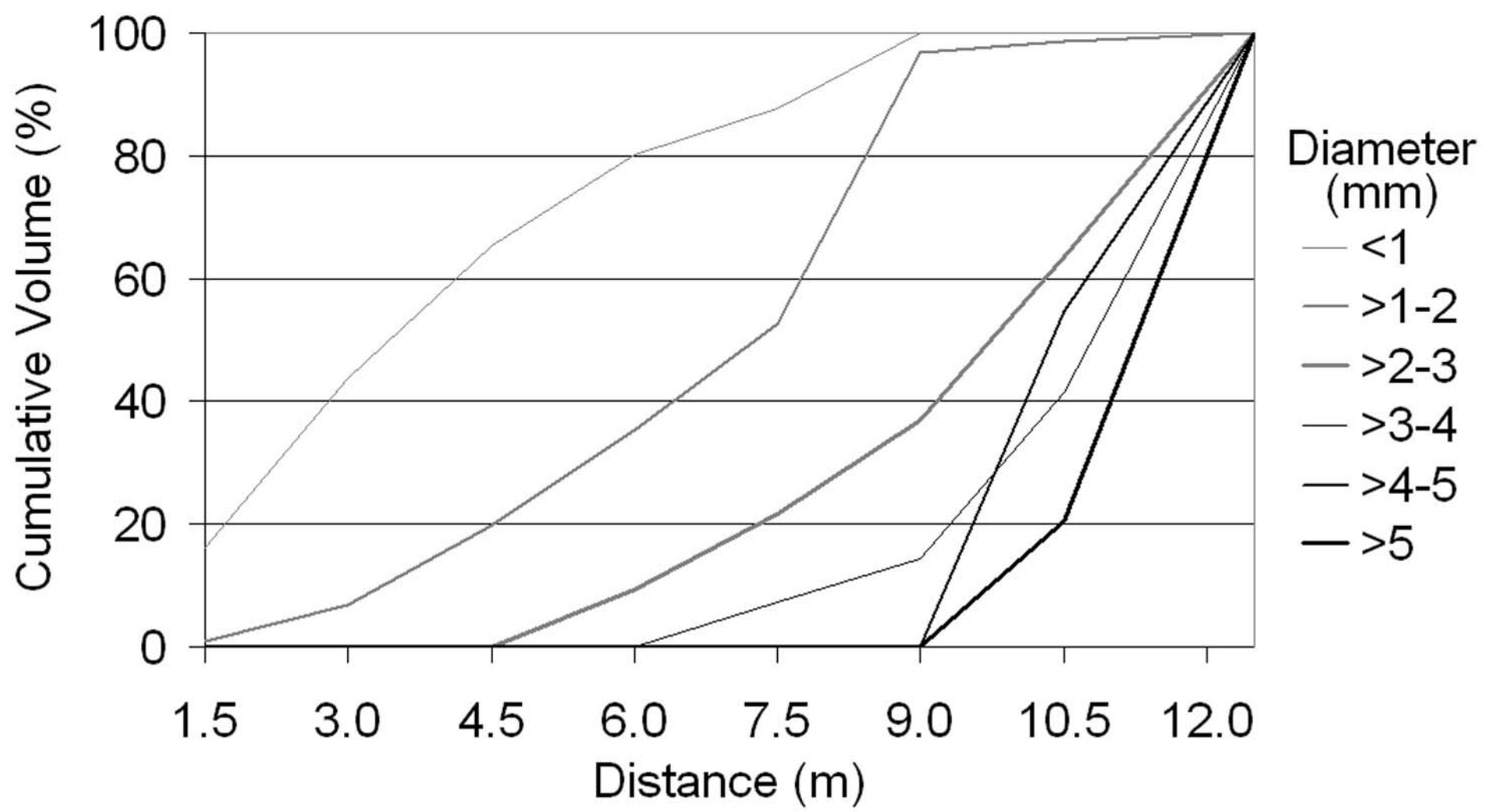
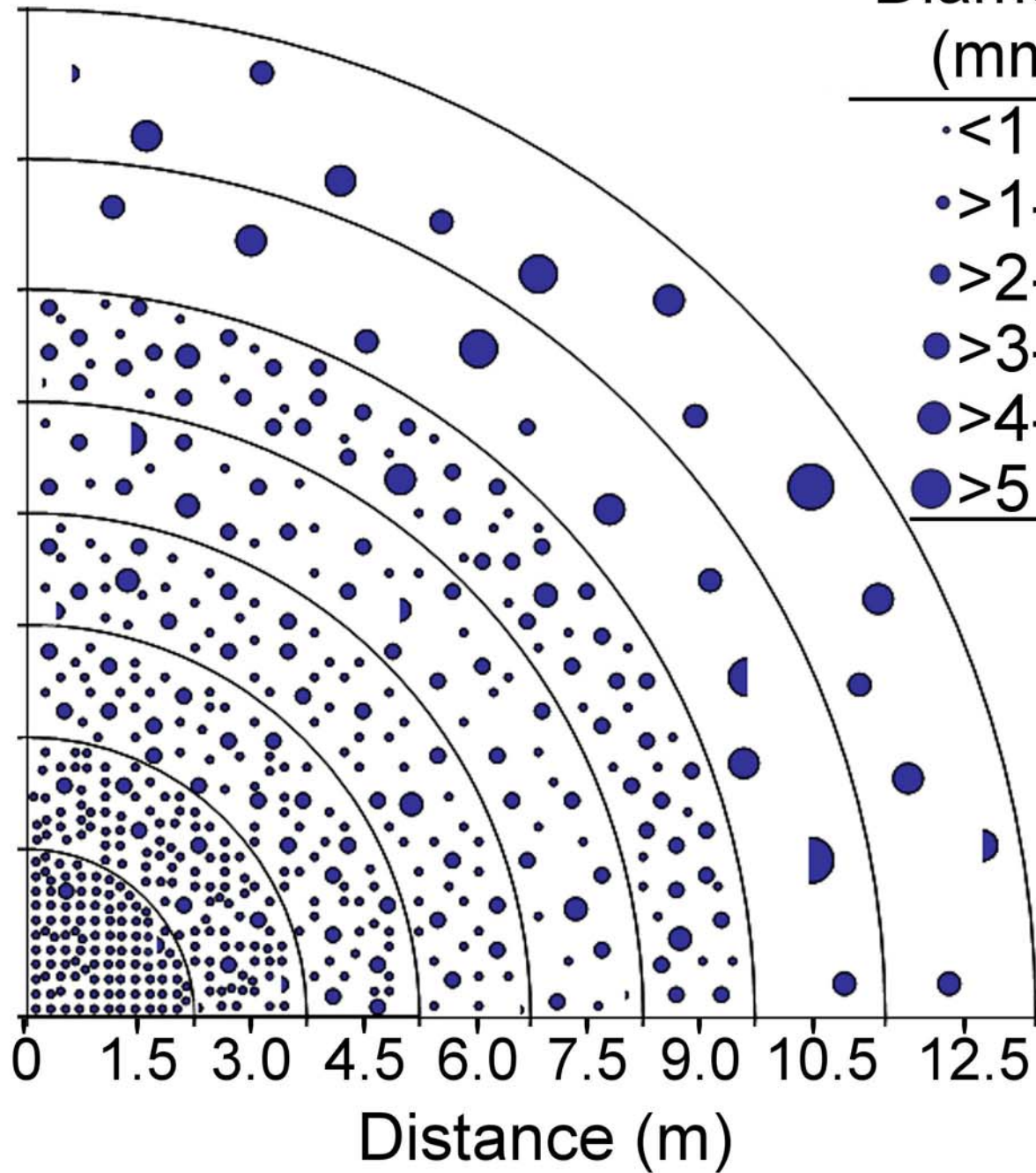


Fig. 11



Diameter (mm)	Frequency (%)	Volume (%)
<1	71.6	7.9
>1-2	22.5	19.6
>2-3	3.3	18.4
>3-4	1.9	27.0
>4-5	0.5	14.1
>5	0.2	13.0

Fig. 12

